Journal of the Operations Research
Society of Japan
Vol. 41, No. 4, December 1998



# DYNAMIC BEHAVIOR OF TCP-LIKE WINDOW CONTROL AND THROUGHPUT PERFORMANCE

Fumio Ishizaki
*The University of Tokushima*

Tetsuya Takine
*Kyoto University*

Yuji Oie
*Kyushu Institute of Technology*

(Received April 30, 1997; Revised October 20, 1997)

*Abstract* In this paper, we consider a TCP-like sliding window control with delayed information. We propose a deterministic fluid-flow queueing system which represents a situation where many TCP connections share a bottleneck link of ATM networks. We provide various properties of the transmission rate function (which is a function of time) to ensure that, with the analytical model, we can compute the throughput performance of TCP over ATM networks. Numerical results show that the synchronization of TCP window control yields heavy degradation of the throughput performance. Further we observe that the throughput is not a continuous function of the peak rate and there exist some regions where the behavior of the throughput has different characteristics. Such complex behavior of the throughput is caused by the complex behavior of the window control.

## 1. Introduction

The performance of TCP (Transmission Control Protocol) over ATM (Asynchronous Transfer Mode) networks is of great interest because a great deal of traffic in future networks is expected to utilize existing transport protocols such as TCP, and TCP is the most widely used transport protocol in today's Internet and private networks [9]. Romanow and Floyd [7] have investigated the performance of TCP over ATM networks without ATM-level congestion control, and compared it to the performance of TCP over conventional packet-based networks. They have shown that the throughput of TCP over ATM networks can be quite low when cells are dropped at a congested ATM switch. They have stated that one of the reasons for the poor performance is the phenomenon that the congested link is occasionally idle due to synchronization of the TCP window control. The poor performance due to the synchronization has also been observed for TCP over conventional packet-based networks in [8]. In this paper, we show not only that the synchronization of TCP window control causes heavy degradation of the throughput performance, but also that the behavior of the synchronization can be very complex.

In the most of the past studies [1, 3, 6, 7], the performance of TCP over ATM networks have been examined by simulations. Contrary to those studies, we develop an analytical model which represents a situation where many TCP connections share a bottleneck link of ATM networks. The model is viewed as a deterministic fluid-flow queueing system which is composed of a finite-buffer queue and a number of sources. Sources use TCP-like sliding window control where information that the window control utilizes is delayed. More precisely, we can interpret our analytical model to represent the following situation: (1) a segment (TCP packet) is fragmented into infinitesimal cells, (2) cells from different segments are completely interleaved at the switch, (3) round trip times (RTTs) are fixed (4) retransmission timers ideally operate and the timeout is always set to 2RTT whenever a source sends data. Items (1) – (4) imply that the synchronization of TCP window control can be

happened so often. However, items (3) and (4) imply that the performance degradation due to the synchronization is restrained at most.

As you will see, our analytical model is described by a system of delay-differential equations or can be regard as a discrete control of continuous-variable system. It is known that the behavior of such systems can be very complex [2, 5]. Pecelli and Kim [5] have examined dynamic behavior of a feedback congestion control scheme, which is similar to a congestion control scheme for available bit rate (ABR) service in ATM networks. In particular, they have considered a simple network model using the feedback control under the presence of delays, which is composed of two sources and an infinite-buffer queue. Their model has been described by delay-differential equations. They have carried out extensive numerical experiments to find parameter values at which orbits presenting dynamics of the feedback control exhibit some noticeable qualitative change. In the numerical experiments, they have shown the existence of complex asymptotic behavior depending on both parameter value and initial condition in an extremely sensitive manner. Finally, they have concluded that even such simple delayed-feedback control models can exhibit complex orbit structure. A similar observation has been made in Chase et al. [2], too.

The remainder of the paper is organized as follows. Section 2 describes our model. In Section 3, we examine the property of the cell transmission rate and provide a theorem which guarantees that we can actually compute dynamics of the system. We also show an algorithm to compute the throughput performance as a function of time. Finally, in section 4, we provide some numerical results which show that the synchronization of TCP window control yields heavy degradation of the throughput performance. We observe that the throughput is not a continuous function of the peak rate and there exist some regions where the behavior of the throughput has different characteristics. The reason for this is two-fold. First, there exist parameter values at which the behavior of the window control exhibit some noticeable qualitative change. For example, the synchronization of the window controls suddenly appears or disappear depending on both peak rates and initial conditions in an extremely sensitive manner. Secondly, the window control strongly governs the throughput performance. Thus, the complex behavior of the window control leads to the complex behavior of the throughput performance.

## 2. Model

We consider a deterministic fluid-flow model composed of a number of sources and a finite-buffer. We denote the buffer size by $B$ (byte). We assume that the $k$th source cannot pour fluid over a peak rate $p^{(k)}$ (byte/sec). It takes the travel time of $\nu^{(k)}$ (sec) for fluid from the $k$th source to reach the buffer. On the other hand, fluid leaks from the buffer at a fixed rate $C$ (byte/sec) as long as fluid remains in the buffer. When the buffer is full, fluid poured into the buffer is lost. The $k$th source receives information about fluid sent from the source with $\tau^{(k)}$ (sec) delay, which we call the delay time of the $k$th source. Received information is utilized by the window control. We assume that $\nu^{(k)}$ and $\tau^{(k)}$ are nonnegative constants. We call $\nu^{(k)} + \tau^{(k)}$ the round trip time (RTT) for the $k$th source.

Before providing the mathematical formulation of the model, we roughly explain the behavior of a source and the window flow control considered in the paper. A source is operated under a sliding window control whose window size is variable and depends on the history of the system. The source continuously pours fluid into the buffer as long as the window control allows it to do so. When the source knows a loss, the source sets the timer which will expire after RTT, while pouring fluid (unless the window is exhausted). Note

that the source ignores the subsequent losses after a loss until it knows the lost fluid is successfully re-poured (as in the Go-back-N ARQ protocol). When the timer expires, the source stops pouring new fluid and re-pours fluid from the lost one as if it would be new fluid, and continues to pour fluid as described above. On the other hand, the window size is determined as follows. When re-pouring due to a loss starts, the window size is set to the segment size $L$. The window control has a (variable) threshold which depends on the history of the window size. If the window size is smaller than the threshold, the window size increases exponentially, and otherwise the window size increases linearly, up to the maximum window size $W$.

Note that the above window flow control is similar to TCP, but not exactly the same. For example, our sources never use fast retransmit and fast recovery algorithms [4, 9] as loss recovery mechanism. In the rest of this section, we provide the mathematical formulation of the model.

Let $a^{(k)}(t)$ denote the transmission rate for the $k$th source at time $t$. $a^{(k)}(t)$ is given by

$$a^{(k)}(t) = \begin{cases} \dfrac{\mathrm{d}^+}{\mathrm{d}t} y^{(k)}(t) & (t \geq 0), \\ 0 & (t < 0), \end{cases} \tag{2.1}$$

where $\mathrm{d}^+/\mathrm{d}t$ denotes a right derivative and $y^{(k)}(t)$, which will be given later, denotes a real function of $t$, which represents the sequence number of fluid that the $k$th source pours at time $t$.

Now we consider the behavior of the queue. Let $q(t)$ denote the amount of fluid in the buffer at time $t$. We assume that $q(t)$ is a continuous function of $t$. $q(t)$ $(t > 0)$ is then given by

$$\frac{\mathrm{d}^+}{\mathrm{d}t} q(t) = \begin{cases} \sum_k a^{(k)}(t - \nu^{(k)}) - C & (0 < q(t) < B), \\ \left[ \sum_k a^{(k)}(t - \nu^{(k)}) - C \right]^- & (q(t) = B), \\ \left[ \sum_k a^{(k)}(t - \nu^{(k)}) - C \right]^+ & (q(t) = 0), \end{cases} \tag{2.2}$$

with initial condition

$$q(0) = q_0 \qquad (q_0 \geq 0),$$

where $[\cdot]^+$ and $[\cdot]^-$ denote $\max(0, \cdot)$ and $\min(0, \cdot)$, respectively.

Let $l^{(k)}(t)$ denote the loss rate for the $k$th source at time $t$. $l^{(k)}(t)$ is given by

$$l^{(k)}(t) = \begin{cases} \dfrac{a^{(k)}(t - \nu^{(k)})}{\sum_m a^{(m)}(t - \nu^{(m)})} \left[ \sum_i a^{(i)}(t - \nu^{(i)}) - C \right]^+ & (q(t) = B, a^{(k)}(t - \nu^{(k)}) > 0), \\ 0 & (\text{otherwise}). \end{cases} \tag{2.3}$$

Let $M^{(k)}(t)$ denote the number of retransmissions by time $t$, where we regards the start of transmission as the first retransmission. We assume that $M^{(k)}(t)$ is a right continuous integer-valued function of $t$ and differentiable except at the finite number of discontinuous points which correspond to the beginning epochs of retransmissions. $M^{(k)}(t)$ is then given by

$$M^{(k)}(t) = M^{(k)}(t-) + 1 \qquad (\theta^{(k)}(t) = 0),$$

$$\frac{\mathrm{d}}{\mathrm{d}t}M^{(k)}(t) = 0 \qquad \text{(otherwise)},$$

with initial condition

$$M^{(k)}(\hat{T}_0^{(k)}) = 1, M^{(k)}(\hat{T}_0^{(k)}-) = 0,$$

where $\hat{T}_0^{(k)} \geq 0$ denotes the beginning epoch of the transmission of the $k$th source and $\theta^{(k)}(t)$ is a right continuous function of $t$ associated with the timer. When $\theta^{(k)}(t)$ reaches zero, a retransmission for the $k$th source starts. $\theta^{(k)}(t)$ is given by

$$\theta^{(k)}(t) = \nu^{(k)} + \tau^{(k)} \qquad (l^{(k)}(t-\tau^{(k)}-) = 0, l^{(k)}(t-\tau^{(k)}) > 0, x^{(k)}(t-) = 1, \theta^{(k)}(t-) < 0),$$

$$\frac{\mathrm{d}}{\mathrm{d}t}\theta^{(k)}(t) = -1 \qquad \text{(otherwise)},$$

with initial condition

$$\theta^{(k)}(t) < 0 \qquad (t \leq 0),$$

where $x^{(k)}(t)$ denotes the state of the $k$th source, which is defined below. Note that $\theta^{(k)}(t) < 0$ implies that the timer is not set.

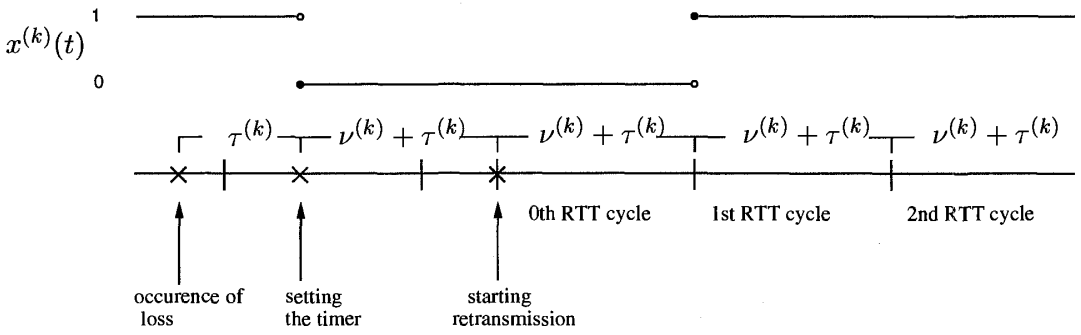


Figure 1: typical behavior of $x^{(k)}(t)$ (success)

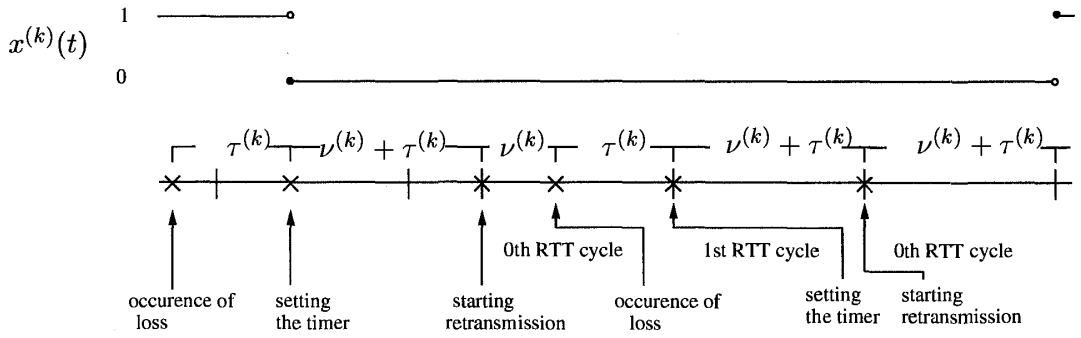


Figure 2: typical behavior of $x^{(k)}(t)$ (failure)

The state $x^{(k)}(t)$ of the $k$th source takes zero during time intervals, each of which starts from an instant when the timer is set and ends at the instant when the $k$th source knows the retransmission of lost fluid succeeds. In other cases, $x^{(k)}(t) = 1$. Thus, $x^{(k)}(t)$ has a downward jump at time $t^*$ when a loss happens at time $t^* - \tau^{(k)}$, and it has a upward jump

at time $t^{**}$ when the retransmission at time $t^{**} - \nu^{(k)} - \tau^{(k)}$ succeeds. We assume $x^{(k)}(t)$ is a right continuous function of $t$ and differentiable except at the finite number of discontinuous points. $x^{(k)}(t)$ $(t \geq 0)$ is then given by

$$x^{(k)}(t) = 1 \qquad (M^{(k)}(t - \nu^{(k)} - \tau^{(k)}) - M^{(k)}(t - \nu^{(k)} - \tau^{(k)}-) > 0, l^{(k)}(t - \tau^{(k)}) = 0),$$

$$x^{(k)}(t) = 0 \qquad (l^{(k)}(t - \tau^{(k)}-) = 0, l^{(k)}(t - \tau^{(k)}) > 0),$$

$$\frac{\mathrm{d}}{\mathrm{d}t}x^{(k)}(t) = 0 \qquad \text{(otherwise)},$$

with initial condition

$$x^{(k)}(t) = 0 \qquad (t < 0).$$

To help readers understand the behavior of $x^{(k)}(t)$, we display typical behavior of $x^{(k)}(t)$ in Figs. 1 and 2 (where RTT cycles will be defined later). Fig. 1 shows $x^{(k)}(t)$ when the retransmission succeeds, while Fig. 2 shows $x^{(k)}(t)$ when the retransmission fails once. Thus our model corresponds to the case that the timeout in TCP for the $k$th source is fixed to $2(\nu^{(k)} + \tau^{(k)})$ $(= 2\mathrm{RTT})$.

Next we consider functions associated with the window control. The sequence number identifies the flow of fluid (which corresponds to the byte of data stream). We use the terminology *sequence number* in this paper, though the sequence number takes a real number in our fluid-flow model. Each source maintains two functions $y^{(k)}(t)$ and $u^{(k)}(t)$ associated with the sequence number, where $y^{(k)}(t)$ and $u^{(k)}(t)$ denote the sequence number of fluid being sent by the $k$th source at time $t$ and the smallest sequence number for transmitted but unacknowledged fluid, respectively. Further, each source maintains two functions $w^{(k)}(t)$ and $h^{(k)}(t)$ associated with the window control, where $w^{(k)}(t)$ and $h^{(k)}(t)$ denote a congestion window and a slow start threshold, (corresponding to the variables usually denoted by *cwnd* and *ssthresh*), respectively, for the $k$th source at time $t$. $u^{(k)}(t)$ $(t \geq 0)$ is given by

$$\frac{\mathrm{d}^+}{\mathrm{d}t}u^{(k)}(t) = \begin{cases} a^{(k)}(t - \nu^{(k)} - \tau^{(k)}) & (x^{(k)}(t) = 1), \\ 0 & (x^{(k)}(t) = 0), \end{cases} \tag{2.4}$$

with initial condition

$$u^{(k)}(t) = 0 \qquad (t < 0).$$

Note that $u^{(k)}(t)$ is a continuous function of $t$. We assume that $y^{(k)}(t)$ is a right continuous function of $t$. $y^{(k)}(t)$ $(t \geq 0)$ is given by

$$y^{(k)}(t) = u^{(k)}(t) \qquad (M^{(k)}(t) - M^{(k)}(t-) > 0),$$

$$\frac{\mathrm{d}^+}{\mathrm{d}t}y^{(k)}(t) = \begin{cases} p^{(k)} & (y^{(k)}(t) < w^{(k)}(t) + u^{(k)}(t)), \\ \min\left(p^{(k)}, \dfrac{\mathrm{d}^+}{\mathrm{d}t}u^{(k)}(t) + \dfrac{\mathrm{d}^+}{\mathrm{d}t}w^{(k)}(t)\right) & (y^{(k)}(t) = w^{(k)}(t) + u^{(k)}(t)), \end{cases} \tag{2.5}$$

with initial condition

$$y^{(k)}(t) = 0 \qquad (t \leq 0).$$

We assume that the congestion window $w^{(k)}(t)$ is a right continuous function of $t$. $w^{(k)}(t)$ is given by

$$w^{(k)}(t) = L \qquad (M^{(k)}(t) - M^{(k)}(t-) > 0),$$

$$\frac{\mathrm{d}^+}{\mathrm{d}t}w^{(k)}(t) = \begin{cases} \dfrac{\mathrm{d}^+}{\mathrm{d}t}u^{(k)}(t) & (w^{(k)}(t) < h^{(k)}(t)), \\ \dfrac{L}{w^{(k)}(t)}\dfrac{\mathrm{d}^+}{\mathrm{d}t}u^{(k)}(t) & (h^{(k)}(t) \le w^{(k)}(t) < W), \\ 0 & (w^{(k)}(t) = W), \end{cases} \tag{2.6}$$

with initial condition

$$w^{(k)}(t) = L \qquad (t \le 0),$$

where $W$ and $L$ ($W > L > 0$) denote the maximum window size and segment size, respectively. Note that, from the definition of $y^{(k)}(t)$, we have $y^{(k)}(t) \le w^{(k)}(t) + u^{(k)}(t)$ for all $t$. We assume that the slow start threshold $h^{(k)}(t)$ is a right continuous function of $t$ and differentiable except at the finite number of discontinuous points. $h^{(k)}(t)$ is given by

$$h^{(k)}(t) = \max\left(\frac{1}{2}w^{(k)}(t-), 2L\right) \qquad (M^{(k)}(t) - M^{(k)}(t-) > 0),$$

$$\frac{\mathrm{d}}{\mathrm{d}t}h^{(k)}(t) = 0 \qquad (\text{otherwise}),$$

with initial condition

$$h^{(k)}(t) = W \qquad (t \le 0).$$

We denote the average throughput at time $t$ for the $k$th source by $S^{(k)}(t)$ ($t > \hat{T}_0^{(k)}$). $S^{(k)}(t)$ is given by

$$S^{(k)}(t) = \frac{u^{(k)}(t)}{t - \hat{T}_0^{(k)}}.$$

Fig. 3 helps readers understand the dependency among the functions defined so far. For example, $x^{(k)}(t)$ is determined by its history, $l^{(k)}(t - \nu^{(k)})$ and $M^{(k)}(t - \nu^{(k)} - \tau^{(k)})$, while $x^{(k)}(t)$ governs $\theta^{(k)}(t)$ and $u^{(k)}(t)$.

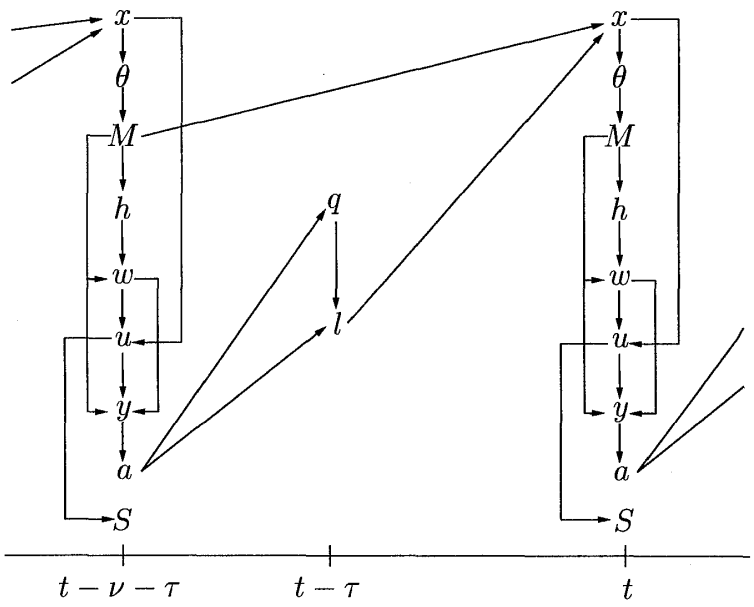


Figure 3: relation between functions

Finally we provide the definitions of retransmission cycles and RTT cycles of the $k$th source. We define the beginning epoch $T_n^{(k)}$ of the $n$th retransmission for the $k$th source as

$$T_0^{(k)} = \hat{T}_0^{(k)},$$

$$T_n^{(k)} = \inf\{t \mid t > T_{n-1}^{(k)}, M^{(k)}(t) - M^{(k)}(t-) > 0\} \qquad (n \geq 1).$$

The open interval $(T_n^{(k)}, T_{n+1}^{(k)})$ is called the $n$th retransmission cycle of the $k$th source. Next we define RTT (round trip time) cycles in a retransmission cycle. Let $T_{m,n}^{(k)}$ denote the beginning epoch of the $n$th RTT cycle in the $m$th retransmission cycle of the $k$th source, where $T_{m,n}^{(k)}$ is given by

$$T_{m,n}^{(k)} = \begin{cases} T_m^{(k)} + n(\nu^{(k)} + \tau^{(k)}) & (0 \leq n < \min\{i \mid T_m^{(k)} + i(\nu^{(k)} + \tau^{(k)}) \geq T_{m+1}^{(k)}\}), \\ T_{m+1}^{(k)} & (n = \min\{i \mid T_m^{(k)} + i(\nu^{(k)} + \tau^{(k)}) \geq T_{m+1}^{(k)}\}). \end{cases}$$

We call the open interval $(T_{m,n}^{(k)}, T_{m,n+1}^{(k)})$ the $(m,n)$-cycle of the $k$th source. If $T_{m,n}^{(k)} + \nu^{(k)} + \tau^{(k)} \leq T_{m+1}^{(k)}$, the $(m,n)$-cycle is called complete cycle. If $T_{m,n}^{(k)} + \nu^{(k)} + \tau^{(k)} > T_{m+1}^{(k)}$, the $(m,n)$-cycle is called interrupted cycle.

We end this section with some properties for retransmission cycles and RTT cycles, which are clear from the definitions of functions involved in those statements.

**Property 2.1** *The length of any retransmission cycle of the kth source is greater than or equal to* $2(\nu^{(k)} + \tau^{(k)})$, *i.e., for any* $n \geq 0$,

$$T_{n+1}^{(k)} - T_n^{(k)} \geq 2(\nu^{(k)} + \tau^{(k)}).$$

**Property 2.2** *In each retransmission cycle,* $w^{(k)}(t)$ *and* $y^{(k)}(t)$ *are right continuous and increasing functions of* $t$. *Further,* $w^{(k)}(t)$ *and* $y^{(k)}(t)$ *are continuous except at* $T_n^{(k)}$*'s* $(n = 0, 1, 2, \cdots)$.

**Property 2.3** *Any retransmission cycle includes at least two complete cycles.*

**Property 2.4** $x^{(k)}(t) = 0$ *for* $T_{m,0}^{(k)} \leq t < T_{m,1}^{(k)}$. *If* $x^{(k)}(t) = 0$ *at some* $t_0 \geq T_{m,1}^{(k)}$, *then* $x^{(k)}(t) = 0$ *for* $t_0 \leq t < T_{m+1,1}^{(k)}$. *In addition, if* $x^{(k)}(t) = 1$, *then there exists a positive number* $\epsilon_0$ *such that if* $0 \leq \epsilon < \epsilon_0$, *then* $x^{(k)}(t + \epsilon) = 1$.

## 3. Analysis

In this section, we will show several results for the properties of the transmission rate function $a^{(k)}(t)$. First, we will show the right continuity of $a^{(k)}(t)$. Second, we will show that the number of discontinuous points of $a^{(k)}(t)$ in each $(m,n)$-cycle is at most one. These results guarantee the existence and the uniqueness of $a^{(k)}(t)$. Thus we can actually compute $a^{(k)}(t)$, and hence dynamics of the system as well as the throughput. In this section, we also provide an algorithm to compute the functions defined so far. In what follows, for simplicity, we use the notation $z_m^{(k)} = z^{(k)}(T_m^{(k)})$ and $z_{m,n}^{(k)} = z^{(k)}(T_{m,n}^{(k)})$ for any function $z^{(k)}(\cdot)$ of $t$.

### 3.1 Analysis of transmission rate function

We first provide a proposition for values which $a^{(k)}(t)$ can take. Combining it with (2.2), we can see that $q(t)$ becomes a piecewise linear function of $t$. Thus, if we can determine $q(t)$ at instants when the value of $a^{(k)}(t)$ changes, we can determine $q(t)$ at any $t$.

**Proposition 3.1** *$a^{(k)}(t)$ takes either 0 or $p^{(k)}$ for all $t$, i.e., $a^{(k)}(t) \in \{0, p^{(k)}\}$ for all $t$.*

The proof is given in Appendix A.1.

Next we provide a proposition for the right continuity of $a^{(k)}(t)$. Combining it with (2.3), we can see that $l^{(k)}(t)$ is a right continuous function of $t$. This will guarantee the right continuity of other functions and their right derivatives as well, e.g., $\theta^{(k)}(t)$, $x^{(k)}(t)$, $\frac{\mathrm{d}^+}{\mathrm{d}t}u^{(k)}(t)$ and so on.

**Proposition 3.2** *$a^{(k)}(t)$ is a right continuous function of $t$. In other words, if $a^{(k)}(t) = p^{(k)}$, there exists a positive number $\epsilon_0$ such that if $0 \leq \epsilon < \epsilon_0$, then $a^{(k)}(t+\epsilon) = p^{(k)}$. Further, if $a^{(k)}(t) = 0$, there exists a positive number $\epsilon_0$ such that if $0 \leq \epsilon < \epsilon_0$, then $a^{(k)}(t+\epsilon) = 0$.*

The proof is given in Appendix A.2.

Next we consider the number of discontinuous points of $a^{(k)}(t)$ in each $(m,n)$-cycle. The proposition will say that the number of discontinuous points of $a^{(k)}(t)$ is finite in any finite interval. Thus, combining with Propositions 3.1 and 3.2, it will guarantee the existence and the uniqueness of $a^{(k)}(t)$, and thereby enabling us to compute $q(t)$ at any $t$.

**Proposition 3.3** *In each $(m,n)$-cycle, $a^{(k)}(t)$ has at most one discontinuous point. If $a^{(k)}(t)$ has a discontinuous point $t_0$ in an $(m,n)$-cycle, then $a^{(k)}(t_0-) = p^{(k)}$ and $a^{(k)}(t_0) = 0$.*

The proof is given in Appendix A.3.

We finally state a theorem, which is a direct conclusion of Propositions 3.1, 3.2 and 3.3.

**Theorem 3.1** *$a^{(k)}(t)$ takes only 0 or $p^{(k)}$ for all $t$ and $a^{(k)}(t)$ is a right continuous function of $t$. In each $(m,n)$-cycle, $a^{(k)}(t)$ has at most one discontinuous point. If $a^{(k)}(t)$ has a discontinuous point $t_0$ in an $(m,n)$-cycle, then $a^{(k)}(t_0-) = p^{(k)}$ and $a^{(k)}(t_0) = 0$.*

### 3.2 Discontinuous points of transmission rate function

In the previous subsection, we proved that $a^{(k)}(t)$ has at most one discontinuous point in each $(m,n)$-cycle. This subsection identifies the discontinuous point in each $(m,n)$-cycle.

**Theorem 3.2** *$a^{(k)}(t)$ has a discontinuous point $t_0$ in an $(m,n)$-cycle such that $a^{(k)}(t_0-) = p^{(k)}$ and $a^{(k)}(t_0) = 0$, if and only if the following conditions are satisfied:*

1. *There exists $\tilde{t}$ such that*

$$\tilde{t} = \min\left\{ t \mid T_{m,n}^{(k)} \leq t < T_{m,n+1}^{(k)}, \frac{\mathrm{d}^+}{\mathrm{d}t}u^{(k)}(t) + \frac{\mathrm{d}^+}{\mathrm{d}t}w^{(k)}(t) = 0 \right\}.$$

2. *There exists $t_1$ such that $f^{(k)}(t_1) = 0$ and $T_{m,n}^{(k)} < t_1 < T_{m,n+1}^{(k)}$.*
3. *If $\tilde{t} = T_{m,n}^{(k)}$, there exists $t_2$ such that $f^{(k)}(t_2) > 0$ and $T_{m,n}^{(k)} < t_2 < T_{m,n+1}^{(k)}$.*

*$t_0$ is then given by*

$$t_0 = \min\left\{ t_1 \mid \tilde{t} \leq t_1, f^{(k)}(t_1) = 0 \right\}, \tag{3.1}$$

*where $f^{(k)}(t) = w^{(k)}(t) + u^{(k)}(t) - w^{(k)}(t)$.*

The proof is given in Appendix A.4.

### 3.3 Numerical algorithm to compute dynamics of the system

In this subsection, we provide a numerical algorithm to compute functions which describe dynamics of the system. Let $\tilde{T}_m^{(k)}$ denote the instant when a loss happens in the $m$th retransmission cycle of the $k$th source, i.e.,

$$\tilde{T}_m^{(k)} = \inf\{t \mid T_m^{(k)} \leq t, l^{(k)}(t) > 0\}.$$

Also, let $\tilde{N}_m^{(k)}$ denote the number of RTT cycles by time $\tilde{T}_m^{(k)}$:

$$\tilde{N}_m^{(k)} = \left\lfloor \frac{\tilde{T}_m^{(k)} - T_{m,0}^{(k)}}{\nu^{(k)} + \tau^{(k)}} \right\rfloor, \tag{3.2}$$

where $\lfloor x \rfloor$ denotes the largest integer that is not greater than $x$. For notational convenience, we define

$$\tilde{t}_m^{(k)} = \tilde{T}_m^{(k)} - T_{m,\tilde{N}_m^{(k)}}^{(k)}. \tag{3.3}$$

Note that the $m$th retransmission cycle of the $k$th source contains $\tilde{N}_m^{(k)} + 2$ RTT cycles, and among them, $\tilde{N}_m^{(k)} + 1$ RTT cycles are complete, while only the last one, whose length may be zero, can be interrupted. In addition, the length of the interrupted cycle is given by $\tilde{t}_m^{(k)}$. Thus we have

$$T_{m+1}^{(k)} = \tilde{T}_m^{(k)} + \nu^{(k)} + 2\tau^{(k)}. \tag{3.4}$$

For $n = 0, \cdots, \tilde{N}_m^{(k)} + 2$, we define $\alpha_{m,n}^{(k)}$ as

$$\alpha_{m,n}^{(k)} = \begin{cases} \sup\{t_0 \mid 0 \le t_0 < T_{m,n+1}^{(k)} - T_{m,n}^{(k)}, a^{(k)}(t_0 + T_{m,n}^{(k)}) = p^{(k)}\} & (a_{m,n}^{(k)} = p^{(k)}), \\ 0 & (a_{m,n}^{(k)} = 0). \end{cases}$$

Also, we define $\delta_{m,n}^{(k)}$ as

$$\delta_{m,n}^{(k)} = \begin{cases} 0 & (n = 0), \\ \alpha_{m,n-1}^{(k)} & (n = 1, \cdots, \tilde{N}_m^{(k)}), \\ \tilde{t}_m^{(k)} & (n = \tilde{N}_m^{(k)} + 1), \\ 0 & (n = \tilde{N}_m^{(k)} + 2). \end{cases} \tag{3.5}$$

Now we rewrite Theorem 3.2 using $\delta_{m,n}^{(k)}$.

**Corollary 3.1** *$a^{(k)}(t)$ has a discontinuous point $t_0$ in an $(m,n)$-cycle such that $a^{(k)}(\hat{t}_{m,n}^{(k)}-) = p^{(k)}$ and $a^{(k)}(\hat{t}_{m,n}^{(k)}) = 0$, if and only if the following conditions are satisfied:*

1. *There exists $t_1$ such that $f^{(k)}(t_1) = 0$ and $T_{m,n}^{(k)} + \delta_{m,n}^{(k)} \le t_1 < T_{m,n+1}^{(k)}$.*
2. *If $\delta_{m,n}^{(k)} = 0$, then $f_{m,n}^{(k)} = w_{m,n}^{(k)} + u_{m,n}^{(k)} - y_{m,n}^{(k)} > 0$.*

*$\hat{t}_{m,n}^{(k)}$ is then given by*

$$\hat{t}_{m,n}^{(k)} = T_{m,n}^{(k)} + (w_{m,n+1}^{(k)} + u_{m,n+1}^{(k)} - y_{m,n}^{(k)})/p^{(k)}.$$

We now show some expressions to keep track of the behavior of the system. We first provide a recursive expression to compute $w_{m,n}^{(k)}$ in terms of $\delta_{m,n}^{(k)}$. From the results in the previous subsection, we obtain, for $n = 0, \ldots, \tilde{N}_m^{(k)} + 1$ ,

$$w_{m,n+1}^{(k)} = \begin{cases} w_{m,n}^{(k)} + \delta_{m,n}^{(k)} p^{(k)} \\ (w_{m,n}^{(k)} + \delta_{m,n}^{(k)} p^{(k)} < h_m^{(k)}), \\ \min\left(\sqrt{2L(\delta_{m,n}^{(k)} p^{(k)} + [w_{m,n}^{(k)} - h_m^{(k)}]^-) + (\max(h_m^{(k)}, w_{m,n}^{(k)}))^2}, W\right) \\ (w_{m,n}^{(k)} + \delta_{m,n}^{(k)} p^{(k)} \ge h_m^{(k)}), \end{cases} \tag{3.6}$$

with initial condition

$$w_{m,0}^{(k)} = L. \tag{3.7}$$

Note that

$$w^{(k)}(T^{(k)}_{m+1,0}-) = w^{(k)}_{m,\tilde{N}^{(k)}_m+2}.$$

Thus we have

$$h^{(k)}_{m+1} = \max\left(\frac{1}{2}w^{(k)}_{m,\tilde{N}^{(k)}_m+2}, 2L\right). \tag{3.8}$$

Also, note that

$$y^{(k)}_{m,n+1} = y^{(k)}_{m,n} + \alpha^{(k)}_{m,n}p^{(k)} \qquad (n \geq 0), \tag{3.9}$$

$$u^{(k)}_{m,n+1} = u^{(k)}_{m,n} + \delta^{(k)}_{m,n}p^{(k)}, \tag{3.10}$$

$$u^{(k)}_{m,0} = y^{(k)}_{m,0}. \tag{3.11}$$

Further, since $\alpha^{(k)}_{m,n} = \min(\hat{t}^{(k)}_{m,n} - T^{(k)}_{m,n}, \nu^{(k)} + \tau^{(k)})$, from (3.9), (3.10) and (3.11), we obtain

$$\alpha^{(k)}_{m,n} = \begin{cases} 0 & (n < 0) \\ \nu^{(k)} + \tau^{(k)} & (n = 0, \cdots, \tilde{N}^{(k)}_m, \alpha^{(k)}_{m,n-1} = \nu^{(k)} + \tau^{(k)}), \\ \min(\frac{1}{p^{(k)}}w^{(k)}_{m,n+1}, \nu^{(k)} + \tau^{(k)}) & (n = 0, \cdots, \tilde{N}^{(k)}_m, \alpha^{(k)}_{m,n-1} < \nu^{(k)} + \tau^{(k)}), \\ \min(\frac{1}{p^{(k)}}w^{(k)}_{m,n+1} + \tilde{t}^{(k)}_m - \alpha^{(k)}_{m,n-1}, \nu^{(k)} + \tau^{(k)}) & (n = \tilde{N}^{(k)}_m + 1), \\ 0 & (n = \tilde{N}^{(k)}_m + 2, \alpha^{(k)}_{m,\tilde{N}^{(k)}_m+1} < \nu^{(k)} + \tau^{(k)}), \\ \frac{1}{p^{(k)}}w^{(k)}_{m,n} + \tilde{t}^{(k)}_m - \alpha^{(k)}_{m,n-1} - \alpha^{(k)}_{m,n-2} & (n = \tilde{N}^{(k)}_m + 2, \alpha^{(k)}_{m,\tilde{N}^{(k)}_m+1} = \nu^{(k)} + \tau^{(k)}). \end{cases} \tag{3.12}$$

Using (3.5), (3.6)–(3.11), we can keep track of the behavior of the system during the $m$th retransmission cycle if we determine $\tilde{T}^{(k)}_m$. Note here that we can determine $\tilde{T}^{(k)}_m$ by tracing $q(t)$. We provide a summary of an algorithm to compute $q(t)$.

**Step 1:** Model Description

Set the values of the number of sources, buffer size $B$, segment size $L$, maximum window size $W$, link capacity $C$ and for all $k$, set the values of travel time $\nu^{(k)}$, delay time $\tau^{(k)}$, peak rate $p^{(k)}$ and the beginning epoch $\hat{T}^{(k)}_0$ of transmission.

**Step 2:** Initialization

Let $t := 0$ and $q(0) := q_0$, and for all $k$, let $m^{(k)} := 0$, $n^{(k)} := 0$, $T^{(k)}_{0,0} := T^{(k)}_0 := \hat{T}^{(k)}_0$, $h^{(k)}_0 := W$, $w^{(k)}_{0,0} := L$, and $\tilde{N}^{(k)}_0 := \tilde{T}^{(k)}_0 := \tilde{t}^{(k)}_0 := T^{(k)}_1 := \infty$.

**Step 3:** Updating variables every RTT cycles

For all $k$, compute $\delta^{(k)}_{m^{(k)},n^{(k)}}$ by (3.5), $w^{(k)}_{m^{(k)},n^{(k)}+1}$ by (3.6) and (3.7), $y^{(k)}_{m^{(k)},n^{(k)}}$ by (3.9), $u^{(k)}_{m^{(k)},n^{(k)}}$ by (3.10) and (3.11), and $\alpha^{(k)}_{m^{(k)},n^{(k)}}$ by (3.12).

**Step 4:** Tracing $q(t)$

Compute

$$t_0 := \min_k\{\underline{t} \mid T^{(k)}_{m^{(k)},n^{(k)}} + \alpha^{(k)}_{m^{(k)},n^{(k)}}-, T^{(k)}_{m^{(k)},n^{(k)}} + \nu^{(k)} + \tau^{(k)}, T^{(k)}_{m^{(k)}+1}+, \underline{t} \geq t\},$$

$$k_0 := \arg\min_k\{\underline{t} \mid T^{(k)}_{m^{(k)},n^{(k)}} + \alpha^{(k)}_{m^{(k)},n^{(k)}}-, T^{(k)}_{m^{(k)},n^{(k)}} + \nu^{(k)} + \tau^{(k)}, T^{(k)}_{m^{(k)}+1}+, \underline{t} \geq t\},$$

where $\arg\min_k$ denotes the argument $k$ attaining the smallest value and

$$q(t_0) := \min\left(\left(q(t) + (\sum_k p^{(k)}\psi^{(k)}_{m^{(k)},n^{(k)}}(t_0) - C)(t - t_0)\right)^+, B\right),$$

where, with an indicator function $I(X)$ of event $X$,

$$\psi^{(k)}_{m^{(k)},n^{(k)}}(t) = I\left(\alpha^{(k)}_{m^{(k)},n^{(k)}} + T^{(k)}_{m^{(k)},n^{(k)}} > t\right).$$

**Step 5:** Buffer overflow
If $q(t) + (\sum_k p^{(k)}\psi^{(k)}_{m^{(k)},n^{(k)}}(t_0) - C)(t - t_0) \geq B$, let $K_l$ be

$$K_l := \{k \mid \psi^{(k)}_{m^{(k)},n^{(k)}} = 1, \tilde{T}^{(k)}_{m^{(k)}} = +\infty\},$$

and for $k \in K_l$,

$$\tilde{T}^{(k)}_{m^{(k)}} := \begin{cases} \dfrac{B - q(t)}{\sum_k p^{(k)}\psi^{(k)}_{m^{(k)},n^{(k)}}(t_0) - C} + t & \left(\sum_k p^{(k)}\psi^{(k)}_{m^{(k)},n^{(k)}}(t_0) - C \neq 0\right), \\ t_0 & \left(\sum_k p^{(k)}\psi^{(k)}_{m^{(k)},n^{(k)}}(t_0) - C = 0\right), \end{cases}$$

and compute $\tilde{N}^{(k)}_{m^{(k)}}$, $\tilde{t}^{(k)}_{m^{(k)}}$ and $T^{(k)}_{m^{(k)}+1}$ by (3.2), (3.3) and (3.4), respectively.
**Step 6:** End of RTT cycle
If $t_0 = T^{(k_0)}_{m^{(k_0)},n^{(k_0)}} + \nu^{(k_0)} + \tau^{(k_0)}$, let $n^{(k_0)} := n^{(k_0)} + 1$.
**Step 7:** End of retransmission cycle
If $t_0 = T^{(k_0)}_{m^{(k_0)}}$, let $m^{(k_0)} := m^{(k_0)} + 1$, $n^{(k_0)} := 0$ and $\tilde{N}^{(k_0)}_{m^{(k_0)}} := \tilde{T}^{(k_0)}_{m^{(k_0)}} := \tilde{t}^{(k_0)}_{m^{(k_0)}} := T^{(k_0)}_{m^{(k_0)}+1} = +\infty$, and then compute $h^{(k_0)}_{m^{(k_0)}}$ by (3.8).
**Step 8** Goto Step 3.

## 4. Numerical Results

In this section, we present some numerical results demonstrating the influence of the peak rate on the throughput of TCP. In the numerical results, we will observe that the synchronization of TCP window control yields heavy degradation of the throughput performance. Through all our numerical results, it is assumed that the segment size $L$ is equal to 512 bytes, the max window size $W$ is equal to 65535 bytes and the link speed $C$ is equal to 150Mbps.

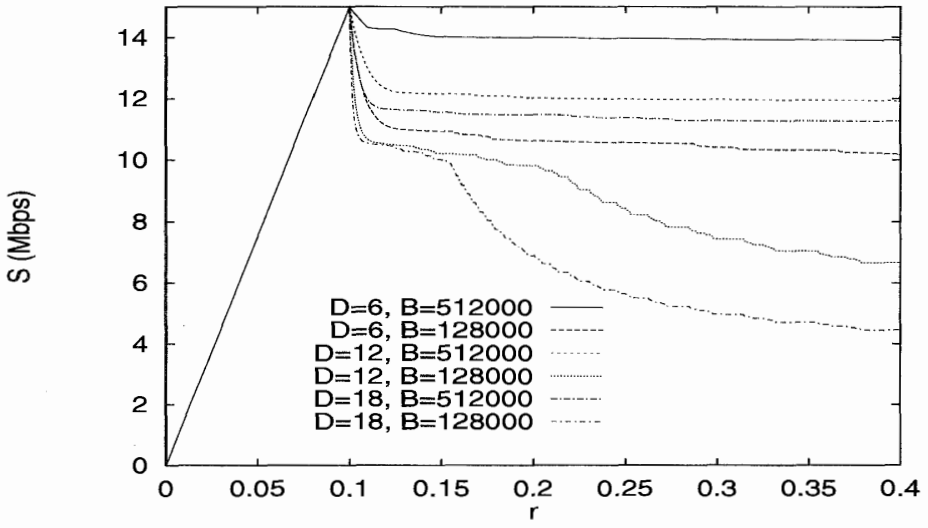


Figure 4: Average throughput of TCP

First, we show the influence of the peak rate on the throughput in homogeneous environments. We assume that 10 TCP connections share a buffer of ATM switch and $q_0 = 0$.

Further, we assume that all the RTTs of TCP connections are the same and the TCP connections are completely synchronized, i.e., $T_0^{(k)} = 0$, $\nu^{(k)} = 0$, $\tau^{(k)} = \tau$ and $p^{(k)} = rC$ for $k = 1, \ldots, 10$. Fig. 4 shows the average throughput during 100 sec as a function of $r$, where $D$ (msec) denotes the length of a RTT and $B$ (byte) denotes the buffer size. For example, $D = 6$, $B = 512000$ indicates that the RTT is equal to 6 msec and the buffer size is equal to 512000 bytes. In Fig. 4, we observe the followings. With the peak rate, the average throughput increases linearly until $r$ reaches 0.1, at which the sum of the peak rates is equal to the link capacity. On the other hand, once $r$ gets larger than 0.1, the average throughput decreases with the increase in the peak rate. In particular, it decreases more rapidly for larger $D$ and smaller $B$.

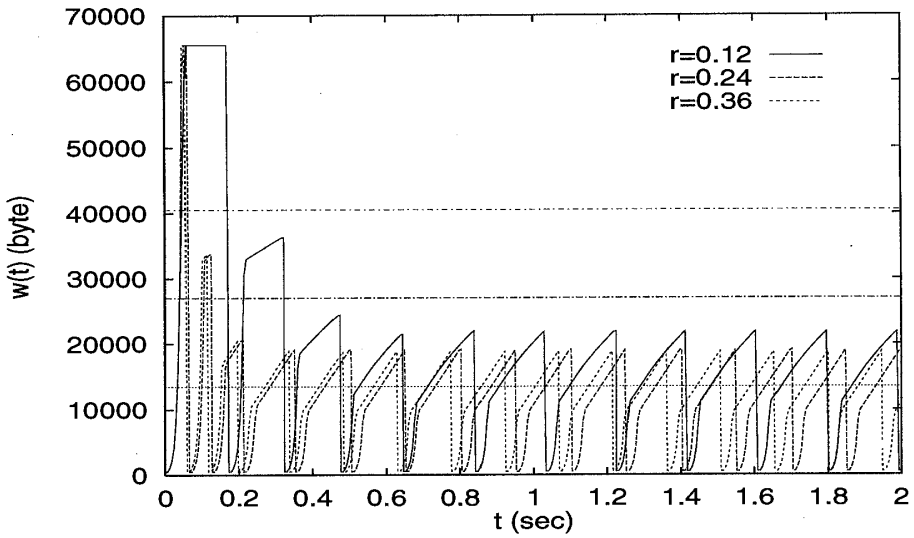


Figure 5: congestion window (D=6,B=512000)

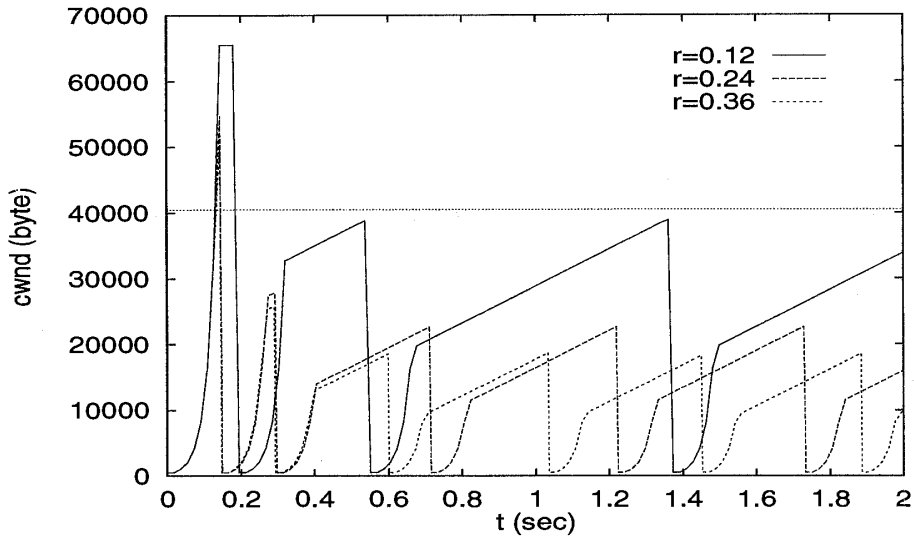


Figure 6: congestion window (D=18,B=128000)

We now examine reasons why the average throughput decreases as the peak rate increases when the sum of the peak rates is greater than the link capacity. For this purpose, we show the dynamic behavior of congestion window $w(t)$ in Figs. 5 and 6. The settings are the same as those in Fig. 4. Note here that $w(t)$ indicates the available window size, so that the maximum amount of data the $k$th source can actually transmit during a RTT of length

$D$ is also limited by $p^{(k)} \times$ RTT . Let $\Theta$ denote RTT $\times$ the peak rate measured in bytes: $\Theta = D \times 150$ (Mb) /8 (b) $\times$ peak rate. With $D = 6$, $\Theta$ is approximately 13500, 27000 and 40500 bytes when $r$ is equal to 0.12, 0.24 and 0.36, respectively. With $D = 18$, $\Theta$ is approximately 40500, 81000 and 121500 bytes when $r$ is equal to 0.12 0.24 and 0.36, respectively. $\Theta$ is also plotted in Figs. 5 and 6.

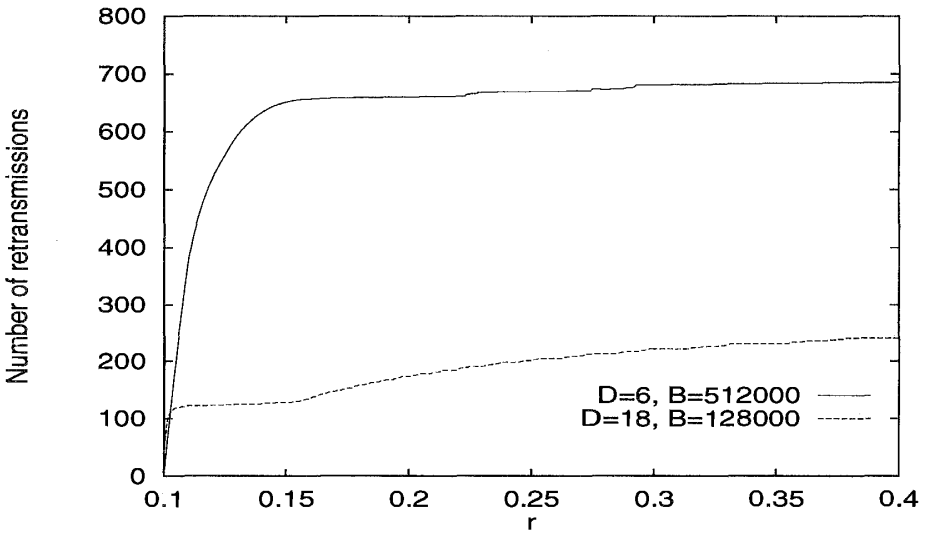


Figure 7: Number of retransmissions

In those figures, we observe that the attained maximum value of $w(t)$ decreases with the increase in $r$. The reason is that the larger the peak rate, the more often packet loss occurs when the peak rate is large. As a result, $w(t)$ cannot increase up to a large value when the peak rate is large. This causes the decrease in the average throughput with the increase in the peak rate when the sum of the peak rates is greater than the link capacity. To confirm that packet loss occurs more often when the peak rate is large, Fig. 7 shows the number of retransmissions due to packet loss during 100sec as a function of the peak rate, where two cases $D = 6, B = 512000$ and $D = 18, B = 128000$ are considered. For both cases, we can see that the number of retransmissions increases with the the peak rate. More precisely, for the case $D = 6, B = 512000$, there is a rapid increase in the number of retransmissions with the peak rate until $r$ gets to 0.14. Once $r$ gets larger than 0.14, the increase becomes very slow. On the other hand, for the case $D = 18, B = 12800$, the interval of the rapid increase is very short. The increase becomes very slow until $r$ gets to 0.16. However, contrary to the case $D = 6, B = 51200$, there is a steady increase in the number of retransmissions when $r$ is over 0.16. This steady increase causes the rapid decrease in the throughput with the increase in the peak rate when $r$ is over 0.16 as shown in Fig. 4.

We observe Figs. 5 and 6 in more detail. In those figures, we can see that the attained maximum value of $w(t)$ decreases with the increase in the peak rate more rapidly when the buffer size is small and the RTT is long. Further, we can observe that, with $D = 6$ and $r = 0.12$, the maximum value of $w(t)$ is greater than $\Theta = 13500$ bytes. As a result, in the case $D = 6, B = 512000$, the throughput does not decrease rapidly with the increase in the peak rate as shown in Fig. 4. On the other hand, with $D = 18, B = 128000$, $w(t)$ is completely below $\Theta$ even when $r = 0.12$. As a result, in the case $D = 18, B = 128000$, the throughput decrease rapidly with the increase in the peak rate as shown in Fig. 4. Thus, when the buffer is small and the length of a RTT is long, TCP window control mechanism cannot prevent the throughput performance from degrading with the increase in the peak

rate.

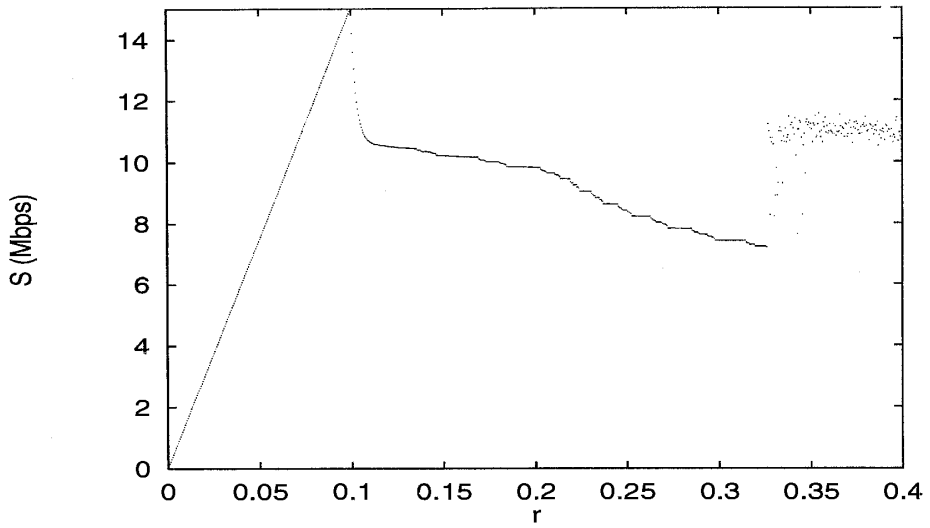


Figure 8: Average throughput of TCP ($T_0^{(k)} = 0$ (msec))

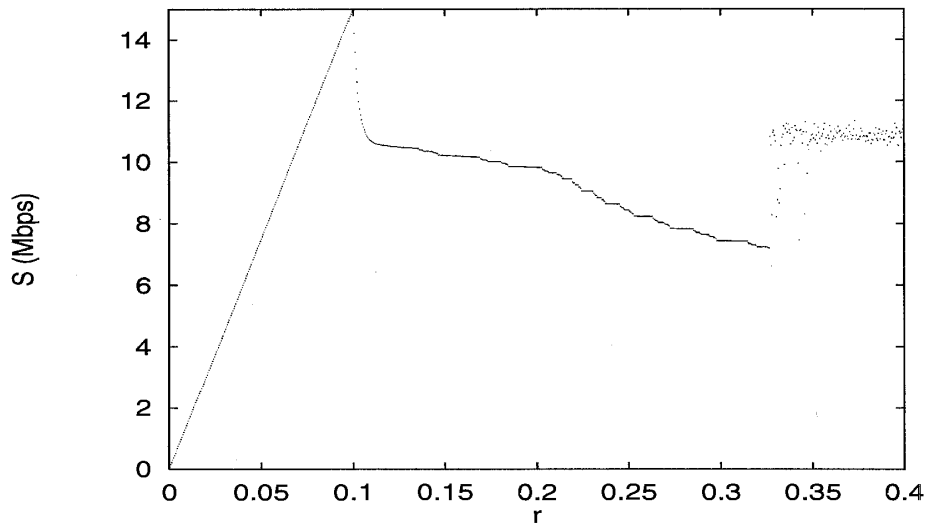


Figure 9: Average throughput of TCP ($T_0^{(k)} = 6$ (msec))

Next, we consider homogeneous environments but not completely synchronized. The setting is the same in the previous case except the beginning epoch $T_0^{(k)}$ of the transmission. We assume that $T_0^{(k)} = 0$ (msec) for $k = 1, \ldots, 5$, $T_0^{(k)} = 6$ (msec) for $k = 6, \ldots, 10$, $D = 12$ and $B = 512000$. Fig. 8 (resp. Fig. 9) shows the average throughput for a source with $T_0^{(k)} = 0$ (resp. $T_0^{(k)} = 6$) during 100 sec as a function of the peak rate $r$. In Figs. 8–9, we observe the followings. First of all, there is a qualitative difference between this case and the synchronized case $D = 12, B = 512000$ given in Fig. 4. When $r$ gets to 0.3270, the average throughput suddenly increases. Once $r$ gets larger than 0.3270, the average throughput shakes irregularly and heavily with the increase in the peak rate.

We examine the reason why such complex behavior of the average throughput is observed. Figs. 10–11 show the dynamic behavior of $w(t)$ for $r = 0.3265$ and $r = 0.3270$, respectively. We observe that the congestion window controls are almost completely synchronized in Fig. 10 (hence, broken lines for $T_0^{(k)} = 6$ may not be seen in this figure), while they are not completely synchronized in Fig. 11. This sensitive dependency on initial conditions

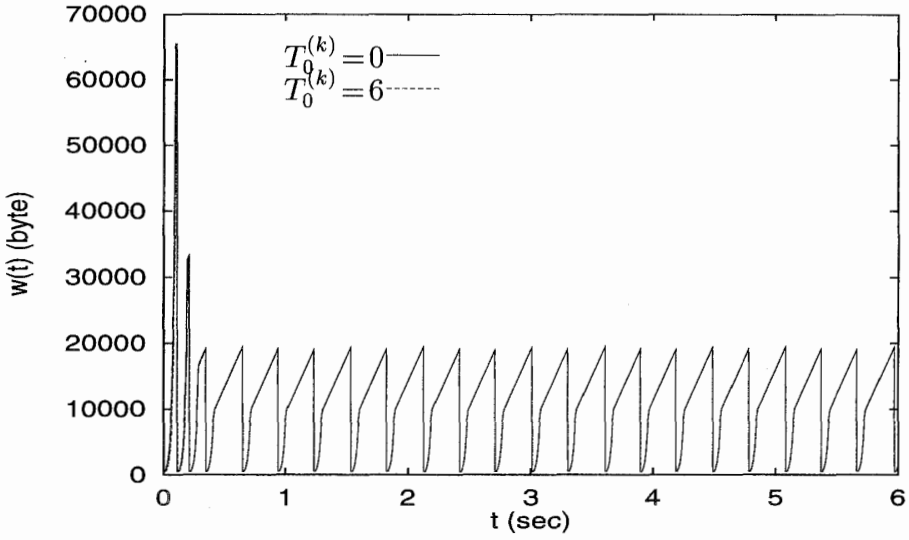


Figure 10: congestion window ($r = 0.3265$)

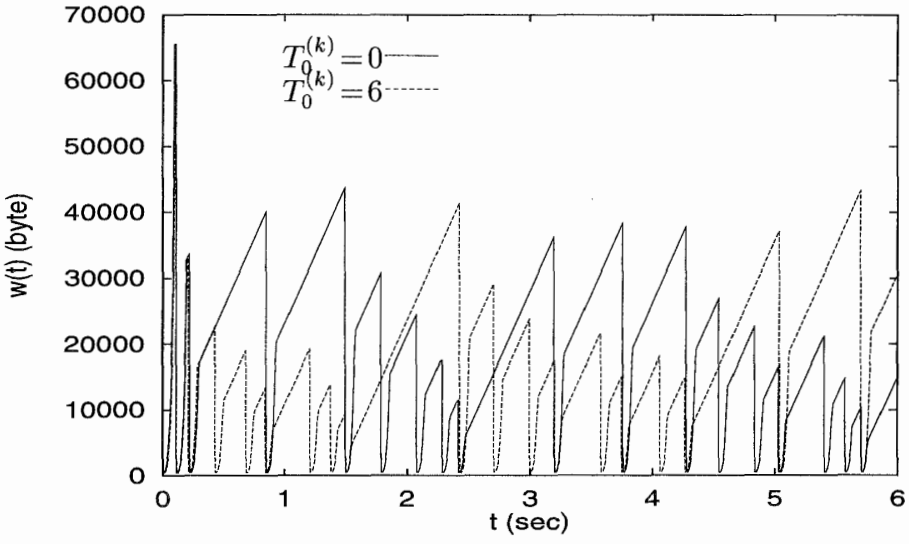


Figure 11: congestion window ($r = 0.3270$)

yields a complex behavior of the average throughput. Indeed, though we do not provide figures because of limitation of space, as far as we examined, in the region $r \in (0.1, 0.3270)$, the window controls for $T_0^{(k)} = 0$ and $T_0^{(k)} = 6$ are almost completely synchronized while dynamics of the window controls are very sensitive to change of peak rates and complex in the region $0.3270 \leq r$. On the other hand, the window controls in Fig. 4 are almost completely synchronized at any peak rates. This suggests that if we can cancel the synchronization of window controls, the throughput performance may be improved in some regions.

Finally, we focus on the heterogeneous case in which TCP connections with different RTTs share the switch. We assume that $q_0 = 0$, $B = 128000$, and for $k = 1, \ldots, 10$, $T_0^{(k)} = 0$, $\nu^{(k)} = 0$, $\tau^{(k)} = \tau$ and $p^{(k)} = rC$. Further, we assume that $\tau^{(k)} = 12$ (msec) for $k = 1, \ldots, 5$ and $\tau^{(k)} = 18$ (msec) for $k = 6, \ldots, 10$, i.e., the length $D$ of RTT of five TCP connections is equal to 12 and that of others is equal to 18. Fig. 12 illustrates the average throughput during 100 sec. When $r$ is not greater than 0.1, the above two groups share the switch in a fair fashion. However, once $r$ gets larger than 0.1, the throughput of

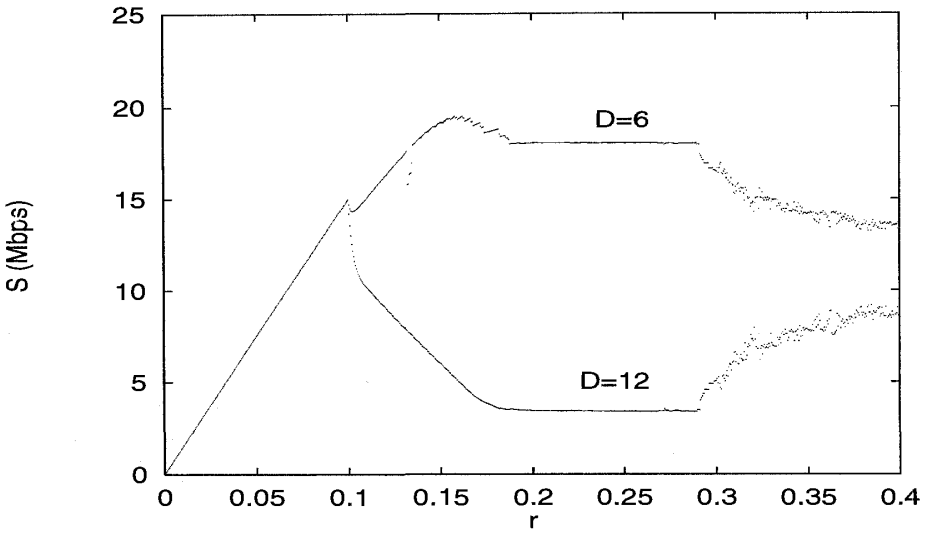


Figure 12: Throughput in the heterogeneous case

TCP connections with long RTTs is heavily degraded with the increase in the peak rate, while the throughput of TCP connections with short RTTs is getting higher. In addition, when $r$ gets to 0.2915, the average throughput of TCP connections with long RTT suddenly increases while that with short RTT suddenly decreases. Thus, the unfairness is somewhat improved in the region $r \geq 0.2915$. Once $r$ gets larger than 0.2915, the average throughput shakes irregularly and heavily with the increase in the peak rate.

We examine the reason why such complex behavior of the average throughput is caused. In Fig. 13 ($r = 0.2910$), we observe that the congestion window controls are completely synchronized, while they are not completely synchronized in Fig. 14 ($r = 0.2915$). Note that $w(t)$ in TCP connections with short RTTs increases more quickly than that in TCP connections with long RTTs because acknowledgments from destinations reach sources more quickly in the former case. Further, packet loss in both of two groups is likely to occur at the same interval because they share the same switch. In fact, if both of two groups send packets when the overflow occurs, packet loss in both of two groups occurs at the same interval. This causes the synchronization of the window controls among two groups. For the above reasons, the attained maximum value of $w(t)$ for $D = 6$ can be larger than that for $D = 12$, as shown in Figs. 13–14. Those observations suggest that if we can cancel the synchronization of window controls, the unfairness may be somewhat improved without degradation of the total throughput performance in some regions.

## A. Proofs

### A.1 Proof of Proposition 3.1

From (2.4) and (2.6), we have

$$\frac{\mathrm{d}^+}{\mathrm{d}t}w^{(k)}(t) = \begin{cases} a^{(k)}(t-\nu^{(k)}-\tau^{(k)}) & (w^{(k)}(t) < h^{(k)}(t), x^{(k)}(t) = 1), \\ \dfrac{L}{w^{(k)}(t)}a^{(k)}(t-\nu^{(k)}-\tau^{(k)}) & (W > w^{(k)}(t) \geq h^{(k)}(t), x^{(k)}(t) = 1), \\ 0 & (x^{(k)}(t) = 0 \text{ or } w^{(k)}(t) = W). \end{cases} \quad \text{(A.1)}$$

Thus, from (2.4) and (A.1), we have

$$\frac{\mathrm{d}^+}{\mathrm{d}t}u^{(k)}(t) + \frac{\mathrm{d}^+}{\mathrm{d}t}w^{(k)}(t) = \gamma^{(k)}(t)a^{(k)}(t-\nu^{(k)}-\tau^{(k)}), \quad \text{(A.2)}$$

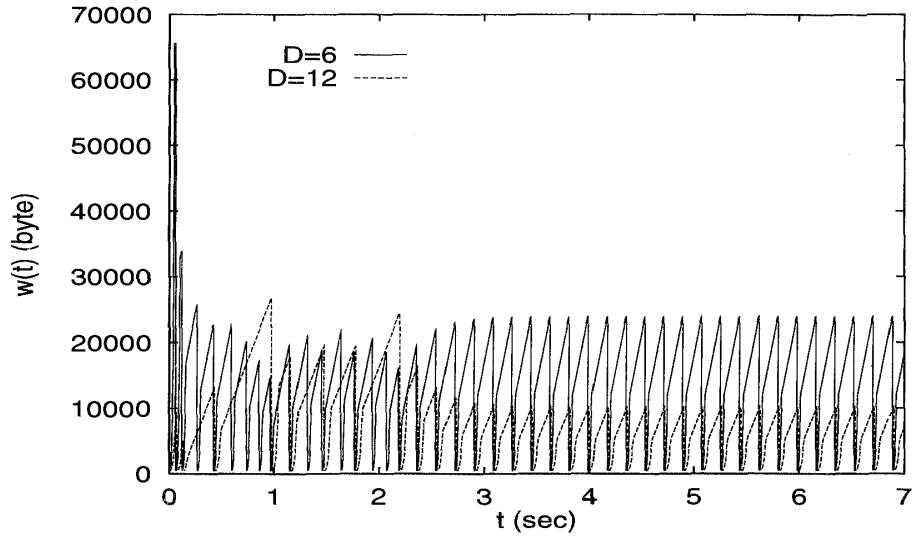


Figure 13: congestion window ($r = 0.2910$)

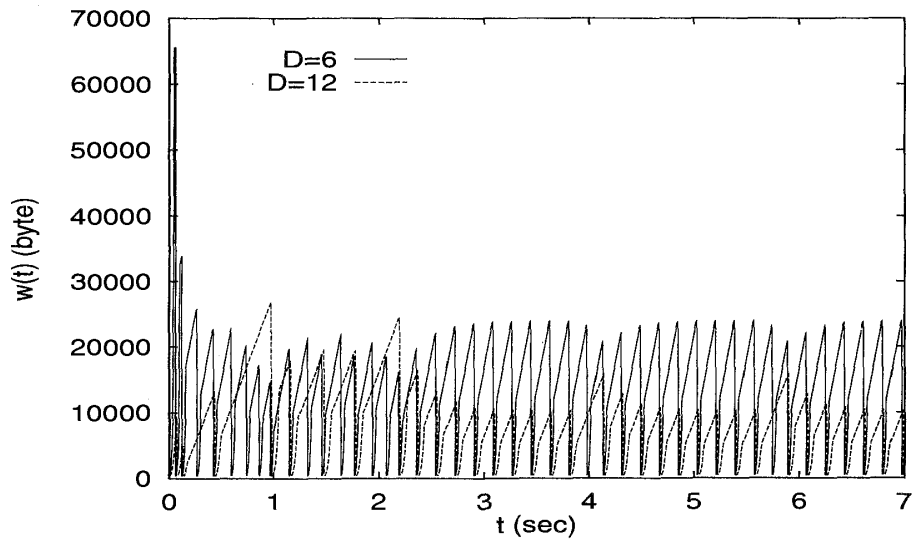


Figure 14: congestion window ($r = 0.2915$)

where $\gamma^{(k)}(t)$ is given by

$$\gamma^{(k)}(t) = \begin{cases} 2 & (w^{(k)}(t) < h^{(k)}(t), x^{(k)}(t) = 1), \\ 1 + \dfrac{L}{w^{(k)}(t)} & (W > w^{(k)}(t) \geq h^{(k)}(t), x^{(k)}(t) = 1), \\ 1 & (w^{(k)}(t) = W, x^{(k)}(t) = 1), \\ 0 & (x^{(k)}(t) = 0). \end{cases} \tag{A.3}$$

From (2.1), (2.5) and (A.2), it follows that for $t \geq 0$

$$a^{(k)}(t) = \begin{cases} p^{(k)} & (f^{(k)}(t) > 0), \\ \min\left(p^{(k)}, \gamma^{(k)}(t) a^{(k)}(t - \nu^{(k)} - \tau^{(k)})\right) & (f^{(k)}(t) = 0), \end{cases} \tag{A.4}$$

where

$$f^{(k)}(t) = w^{(k)}(t) + u^{(k)}(t) - y^{(k)}(t). \tag{A.5}$$

From (A.4), it follows that, for any fixed $t \geq 0$, if $a^{(k)}(t - \nu^{(k)} - \tau^{(k)})$ takes either 0 or $p^{(k)}$, $a^{(k)}(t)$ also takes either 0 or $p^{(k)}$. Thus, from (2.1), we see that $a^{(k)}(t)$ takes either 0 or $p^{(k)}$

for $0 \leq t \leq \nu^{(k)} + \tau^{(k)}$. Using this and (A.4) recursively and noting (A.3), we conclude that $a^{(k)}(t)$ takes either 0 or $p^{(k)}$ for all $t$.

### A.2 Proof of Proposition 3.2

From Proposition 3.1 and (A.4), we obtain

$$a^{(k)}(t) = \begin{cases} p^{(k)} & (f^{(k)}(t) > 0), \\ p^{(k)} & (f^{(k)}(t) = 0, x^{(k)}(t) = 1, a^{(k)}(t - \nu^{(k)} - \tau^{(k)}) = p^{(\kappa)}), \\ 0 & (f^{(k)}(t) = 0, x^{(k)}(t) = 1, a^{(k)}(t - \nu^{(k)} - \tau^{(k)}) = 0), \\ 0 & (f^{(k)}(t) = 0, x^{(k)}(t) = 0). \end{cases}$$

**Property A.5** *$f^{(k)}(t)$ is right continuous at every $t$. Further, $f^{(k)}(t)$ is continuous except at $T_m^{(k)}$'s $(m = 0, 1, 2, \cdots)$.*

From Proposition 3.1, (2.5), (A.2), (A.4) and (A.5), we have for $t > 0$

$$f^{(k)}(t) = L \qquad (t = T_m^{(k)}; m = 0, 1, 2, \cdots), \tag{A.6}$$

$$\frac{\mathrm{d}^+}{\mathrm{d}t} f^{(k)}(t) = \begin{cases} \gamma^{(k)}(t) a^{(k)}(t - \nu^{(k)} - \tau^{(k)}) - p^{(k)} & (f^{(k)}(t) > 0), \\ \left[\gamma^{(k)}(t) a^{(k)}(t - \nu^{(k)} - \tau^{(k)}) - p^{(k)}\right]^+ & (f^{(k)}(t) = 0), \end{cases} \tag{A.7}$$

with initial condition

$$f^{(k)}(t) = L \qquad (t \leq 0).$$

From Property A.5 and (A.7), we see that $f^{(k)}(t) \geq 0$ for all $t$. Let $\pi^{(k)}(t)$ denote the state of the window control for the $k$th source. $\pi^{(k)}(t)$ is given by

$$\pi^{(k)}(t) = \begin{cases} 1 & (f^{(k)}(t) > 0), \\ 2 & (f^{(k)}(t) = 0, x^{(k)}(t) = 1, a^{(k)}(t - \nu^{(k)} - \tau^{(k)}) = p^{(k)}), \\ 3 & (f^{(k)}(t) = 0, x^{(k)}(t) = 1, a^{(k)}(t - \nu^{(k)} - \tau^{(k)}) = 0), \\ 4 & (f^{(k)}(t) = 0, x^{(k)}(t) = 0). \end{cases} \tag{A.8}$$

We then have

$$a^{(k)}(t) = \begin{cases} p^{(k)} & (\pi^{(k)}(t) \in \{1, 2\}), \\ 0 & (\pi^{(k)}(t) \in \{3, 4\}). \end{cases} \tag{A.9}$$

For notational convenience, we denote a transition from state $i$ to state $j$ by a transition $ij$ $(i, j = 1, 2, 3, 4)$.

**Lemma A.1**

1. *If $\pi^{(k)}(t) = 1$, there exists a positive number $\epsilon_0$ such that if $0 \leq \epsilon < \epsilon_0$, then $\pi^{(k)}(t+\epsilon) = 1$.*
2. *If $\pi^{(k)}(t) = 2$, there exists a positive number $\epsilon_0$ such that if $0 \leq \epsilon < \epsilon_0$, then $\pi^{(k)}(t+\epsilon) = 1$ or $\pi^{(k)}(t + \epsilon) = 2$.*
3. *If $\pi^{(k)}(t) = 3$, there exists a positive number $\epsilon_0$ such that if $0 \leq \epsilon < \epsilon_0$, then $\pi^{(k)}(t+\epsilon) = 3$.*
4. *If $\pi^{(k)}(t_0) = 4$ at some $t_0 \geq T_{m,1}^{(k)}$, then $\pi^{(k)}(t) = 4$ for $t_0 \leq t < T_{m+1}^{(k)}$.*

PROOF:

1. From Property A.5, it is clear.
2. From Properties 2.4, A.5, (A.3) and (A.7), it is clear.
3. From Properties 2.4, A.5, (A.3) and (A.7), it is clear.

4. Since $x^{(k)}(t_0) = 0$, from Property 2.4, we see that $x^{(k)}(t) = 0$ for $t_0 \leq t < T^{(k)}_{m+1,1}$. Thus, from (A.3), we have $\gamma^{(k)}(t) = 0$ for $t_0 \leq t < T^{(k)}_{m+1,1}$. From (A.7), (A.9) and Property A.5, we see that $f^{(k)}(t) = 0$ for $t_0 \leq t < T^{(k)}_{m+1}$, which completes the proof. ∎

Thus, Proposition 3.2 follows from Lemma A.1, (A.8) and (A.9).

### A.3 Proof of Proposition 3.3

To prove Proposition 3.3, we need several lemmas.

**Lemma A.2** *If $f^{(k)}(t_1) = 0$ and $f^{(k)}(t_2) > 0$ for some $t_1 < t_2$ in an $(m, n)$-cycle, there exists some $t_0$ $(t_1 \leq t_0 < t_2)$ such that $a^{(k)}(t_0 - \nu^{(k)} - \tau^{(k)}) = p^{(k)}$.*

PROOF: We assume that $f^{(k)}(t_1) = 0$ and $f^{(k)}(t_2) > 0$ for some $t_1 < t_2$ in an $(m, n)$-cycle. From Proposition 3.1, Property A.5 and (A.7), it then follows that there exists some $t_0$ such that $a^{(k)}(t_0 - \nu^{(k)} - \tau^{(k)}) = p^{(k)}$ and $t_1 \leq t_0 < t_2$. ∎

**Lemma A.3**

1. *If $\pi^{(k)}(t_1) = 3$ and $\pi^{(k)}(t_2) = 1$ for some $t_1 < t_2$ in an $(m, n+1)$-cycle $(m, n \geq 0)$, then $a^{(k)}(t)$ has a discontinuous point $t_0$ in the $(m, n)$-cycle such that $a^{(k)}(t_0-) = 0, a^{(k)}(t_0) = p^{(k)}$ and $t_1 - \nu^{(k)} - \tau^{(k)} < t_0 \leq t_2 - \nu^{(k)} - \tau^{(k)}$.*
2. *If $\pi^{(k)}(t_1-) = 3$ and $\pi^{(k)}(t_1) = 2$ for some $t_1$ in an $(m, n+1)$-cycle $(m, n \geq 0)$, then $a^{(k)}(t)$ has a discontinuous point $t_0$ in the $(m, n)$-cycle such that $a^{(k)}(t_0-) = 0$, $a^{(k)}(t_0) = p^{(k)}$ and $t_0 = t_1 - \nu^{(k)} - \tau^{(k)}$.*

PROOF: First we will prove the first part of Lemma A.3. Since $\pi^{(k)}(t_1) = 3$ and $\pi^{(k)}(t_2) = 1$ for some $t_1 < t_2$ in an $(m, n+1)$-cycle $(m, n \geq 0)$, from (A.8) we have $f^{(k)}(t_1) = 0$ and $f^{(k)}(t_2) > 0$. Thus, from Lemma A.2, there exists some $t_3$ $(t_1 \leq t_3 < t_2)$ such that $a^{(k)}(t_3 - \nu^{(k)} - \tau^{(k)}) = p^{(k)}$. On the other hand, since $\pi^{(k)}(t_1) = 3$, from (A.8) we have $a^{(k)}(t_1 - \nu^{(k)} - \tau^{(k)}) = 0$. From Propositions 3.1 and 3.2, we therefore conclude that $a^{(k)}(t)$ has a discontinuous point $t_0$ in the $(m, n)$-cycle such that $a^{(k)}(t_0-) = 0, a^{(k)}(t_0) = p^{(k)}$ and $t_1 - \nu^{(k)} - \tau^{(k)} < t_0 \leq t_3 - \nu^{(k)} - \tau^{(k)}$, which proves the first part.

Next we will prove the second part. From (A.8), we have $a^{(k)}(t_1 - \nu^{(k)} - \tau^{(k)}-) = 0$ and $a^{(k)}(t_1 - \nu^{(k)} - \tau^{(k)}) = p^{(k)}$. ∎

**Lemma A.4** *If $a^{(k)}(t)$ has a discontinuous point $t_1$ in an $(m, n+1)$-cycle $(m, n \geq 0)$ such that $a^{(k)}(t_1-) = 0$ and $a^{(k)}(t_1) = p^{(k)}$, $a^{(k)}(t)$ has a discontinuous point $t_0$ in the $(m, n)$-cycle such that $a^{(k)}(t_0-) = 0$ and $a^{(k)}(t_0) = p^{(k)}$.*

PROOF: If $a^{(k)}(t)$ has a discontinuous point $t_1$ in an $(m, n+1)$-cycle such that $a^{(k)}(t_1-) = 0$ and $a^{(k)}(t_1) = p^{(k)}$, from (A.8) and (A.9), we see that one of the following state transitions must occur at $t_1$: transitions 31, 32, 41 or 42. From Lemma A.1, the transitions 41 and 42 can not occur at $t_1$. On the other hand, from Lemma A.3, if the transitions 31 or 32 occur at $t_1$, then $a^{(k)}(t)$ has a discontinuous point $t_0$ in the $(m, n)$-cycle such that $a^{(k)}(t_0-) = 0$ and $a^{(k)}(t_0) = p^{(k)}$. ∎

**Lemma A.5** *If $a^{(k)}(t)$ does not have a discontinuous point in an $(m, n)$-cycle $(m, n \geq 0)$ such that $a^{(k)}(t_0-) = 0$ and $a^{(k)}(t_0) = p^{(k)}$, then $a^{(k)}(t)$ has at most one discontinuous point in the $(m, n+1)$-cycle. Further, if $a^{(k)}(t)$ has exactly one discontinuous point $t_1$ in the $(m, n+1)$-cycle, then $a^{(k)}(t_1-) = p^{(k)}$ and $a^{(k)}(t_1) = 0$.*

PROOF: To prove the first part of the lemma, we prove its contraposition. Suppose that $a^{(k)}(t)$ has more than one discontinuous point in an $(m, n+1)$-cycle. Then, from Propositions 3.1 and 3.2, $a^{(k)}(t)$ has at least one discontinuous point in the $(m, n+1)$-cycle such that $a^{(k)}(t_0-) = 0$ and $a^{(k)}(t_0) = p^{(k)}$. Thus, from Lemma A.4, $a^{(k)}(t)$ has a discontinuous point in the $(m, n)$-cycle such that $a^{(k)}(t_0-) = 0$ and $a^{(k)}(t_0) = p^{(k)}$, which proves the first part.

We next prove the second part of the lemma. From Lemma A.4, if $a^{(k)}(t)$ does not have a discontinuous point in an $(m, n)$-cycle such that $a^{(k)}(t_0-) = 0$ and $a^{(k)}(t_0) = p^{(k)}$, then $a^{(k)}(t)$ does not have a discontinuous point $t_1$ in the $(m, n+1)$-cycle such that $a^{(k)}(t_1-) = 0$ and $a^{(k)}(t_1) = p^{(k)}$. Note that, from Theorem 3.1, there are only two kinds of the discontinuous points: (i) $a^{(k)}(t_0-) = 0$, $a^{(k)}(t_0) = p^{(k)}$ and (ii) $a^{(k)}(t_0-) = p^{(k)}$, $a^{(k)}(t_0) = 0$. Therefore if $a^{(k)}(t)$ has exactly one discontinuous point $t_1$ in the $(m, n+1)$-cycle, $a^{(k)}(t_1-) = p^{(k)}$ and $a^{(k)}(t_1) = 0$. ∎

**Lemma A.6** *If $x^{(k)}(t) = 0$ for $T_m^{(k)} \le t_0 \le t < t_1 \le T_{m+1}^{(k)}$ and $f^{(k)}(t_0) = 0$, then $a^{(k)}(t) = 0$ and $f^{(k)}(t) = 0$ for $t_0 \le t < t_1$.*

PROOF: Since $x^{(k)}(t) = 0$ for $t_0 \le t < t_1$ and $f^{(k)}(t_0) = 0$, from (A.3) and (A.7), we have $f^{(k)}(t) = 0$ for $t_0 \le t < t_1$. From (A.8), we therefore have $\pi^{(k)}(t) = 4$ for $t_0 \le t < t_1$. Thus, from (A.9), we obtain $a^{(k)}(t) = 0$ for $t_0 \le t < t_1$. ∎

**Lemma A.7** *$a^{(k)}(t)$ does not have a discontinuous point in an $(m, 0)$-cycle ($m \ge 0$) such that $a^{(k)}(t_0-) = 0$ and $a^{(k)}(t_0) = p^{(k)}$.*

PROOF: From Property A.5 and (A.6), there exists a positive number $\epsilon_0$ such that if $0 \le \epsilon < \epsilon_0$, $f^{(k)}(T_m^{(k)} + \epsilon) > 0$, and hence $\pi^{(k)}(T_m^{(k)} + \epsilon) = 1$ and $a^{(k)}(T_m^{(k)} + \epsilon) = p^{(k)}$. Thus, from Lemma A.6 and Property 2.4, $a^{(k)}(t)$ has at most one discontinuous point in an $(m, 0)$-cycle. In addition, if $a^{(k)}(t)$ has a discontinuous point $t_0$ in the $(m, 0)$-cycle, $a^{(k)}(t_0-) = p^{(k)}$ and $a^{(k)}(t_0) = 0$. ∎

Proposition 3.3 now follows from repeated arguments with Lemmas A.5 and Lemma A.7.

### A.4 Proof of Theorem 3.2

To prove the theorem, we need three lemmas.

**Lemma A.8** $\frac{d^+}{dt}u^{(k)}(t) + \frac{d^+}{dt}w^{(k)}(t)$ *is right continuous and* $\frac{d^+}{dt}u^{(k)}(t) + \frac{d^+}{dt}w^{(k)}(t) \ge 0$. *Further,* $\frac{d^+}{dt}u^{(k)}(t) + \frac{d^+}{dt}w^{(k)}(t)$ *is decreasing in each $(m, n)$-cycle.*

PROOF: The lemma follows from (A.2) and (A.3), Properties 2.2 and 2.4, and Theorem 3.1. ∎

**Lemma A.9** $\frac{d^+}{dt}u^{(k)}(t) + \frac{d^+}{dt}w^{(k)}(t) = 0$ *if and only if* $a^{(k)}(t - \nu^{(k)} - \tau^{(k)}) = 0$ *or* $x^{(k)}(t) = 0$.

PROOF: From (A.2) and (A.3), it is clear. ∎

We now prove the only if part of Theorem 3.2. From Theorem 3.1, one of the state transitions 13, 14, 23 or 24 must occur at $t_0$ and no other transitions occur in an $(m, n)$-cycle.

Assume that transitions 13 or 14 occur at $t_0$ in the $(m, n)$-cycle. From Lemma A.9, (A.8) and the assumption, $\frac{d^+}{dt}u^{(k)}(t_0) + \frac{d^+}{dt}w^{(k)}(t_0) = 0$. Thus, the condition 1 is satisfied. Also,

from the assumption, it is clear that the conditions 2 and 3 are satisfied. Next we will show $t_0$ is given by (3.1). In this case, from Lemma A.9 and (A.8), we have $f(t_0-) > 0$, $f(t_0) = 0$ and $\frac{\mathrm{d}^+}{\mathrm{d}t}u^{(k)}(t_0) + \frac{\mathrm{d}^+}{\mathrm{d}t}w^{(k)}(t_0) = 0$. Thus, it is sufficient to show that there does not exist $t_1$ such that $f^{(k)}(t_1) = 0$ and $\tilde{t} \le t_1 < t_0$. Suppose that there exists such $t_1$. Since $\tilde{t} \le t_1$, from Lemma A.8, we have $\frac{\mathrm{d}^+}{\mathrm{d}t}u^{(k)}(t_1) + \frac{\mathrm{d}^+}{\mathrm{d}t}w^{(k)}(t_1) = 0$. From Lemma A.9, this implies $x^{(k)}(t_1) = 0$ or $a^{(k)}(t_1 - \nu^{(k)} - \tau^{(k)}) = 0$. Further, from the assumption, we have $f^{(k)}(t_1) = 0$. Therefore we obtain $a^{(k)}(t_1) = 0$. On the other hand, from Theorem 3.1, we know that $a^{(k)}(t) = p^{(k)}$ for every $t$ such that $T^{(k)}_{m,n} < t < t_0$. Those are contradictions. Therefore, there does not exist $t_1$ such that $f^{(k)}(t_1) = 0$ and $\tilde{t} \le t_1 < t_0$. $t_0$ is thus given by (3.1).

Assume that transitions 23 or 24 occur at $t_0$ in the $(m,n)$-cycle. From Lemma A.9, (A.8) and the assumption, there exists $t_3$ such that $\frac{\mathrm{d}^+}{\mathrm{d}t}u^{(k)}(t_3) + \frac{\mathrm{d}^+}{\mathrm{d}t}w^{(k)}(t_3) = 0$. Thus, the condition 1 is satisfied. Also, from the assumption, it is clear that the condition 2 is satisfied. Note that $\tilde{t} \neq T^{(k)}_{m,n}$ in this case. To prove this, we assume that $\tilde{t} = T^{(k)}_{m,n}$ From Lemmas A.8 and A.9, we have $a^{(k)}(t - \nu^{(k)} - \tau^{(k)}) = 0$ or $x^{(k)}(t) = 0$ for every $t$ such that $T^{(k)}_{m,n} \le t < T^{(k)}_{m,n+1}$. On the other hand, from the assumption, we have $a^{(k)}(t_0 - \nu^{(k)} - \tau^{(k)}) = 0$ and $x^{(k)}(t_0) = 0$. Those are contradictions. Therefore, we conclude that $\tilde{t} \neq T^{(k)}_{m,n}$ in this case. Thus, the condition 3 is satisfied. Further, from Lemma A.9 and (A.8), $t_0$ is given by (3.1).

Next we prove the if part. From Theorem 3.1, it is sufficient to show $a^{(k)}(t_0-) = p^{(k)}$ and $a^{(k)}(t_0) = 0$. We consider the two cases separately: (i) $T^{(k)}_{m,n} < \tilde{t} < T^{(k)}_{m,n+1}$, and (ii) $\tilde{t} = T^{(k)}_{m,n}$.

In the case (i), from Lemma A.8, we have $\frac{\mathrm{d}^+}{\mathrm{d}t}u^{(k)}(t_2) + \frac{\mathrm{d}^+}{\mathrm{d}t}w^{(k)}(t_2) = 0$ for every $t_2$ such that $\tilde{t} \le t_2 < T^{(k)}_{m,n+1}$. Since $f^{(k)}(t_0) = 0$ and $\tilde{t} \le t_0$ from (3.1), we obtain $a^{(k)}(t_0) = 0$ from Lemma A.9, (A.8) and (A.9). To show $a^{(k)}(t_0-) = p^{(k)}$, we consider the two cases separately: (a) $\tilde{t} < t_0$, and (b) $\tilde{t} = t_0$. In the case (a), from Property A.5, we have $f^{(k)}(t_2) > 0$ for every $t_2$ such that $\tilde{t} \le t_2 < t_0$. Thus, from Theorem 3.1, (A.8) and (A.9), we have $a^{(k)}(t_0-) = p^{(k)}$. In the case (b), from Lemma A.8 and the condition 1, we have $\frac{\mathrm{d}^+}{\mathrm{d}t}u^{(k)}(t_0-) + \frac{\mathrm{d}^+}{\mathrm{d}t}w^{(k)}(t_0-) > 0$. Note here that, from the assumption (i), $t_0 \neq T^{(k)}_{m,n}$ in this case. From Theorem 3.1, Lemma A.9, (A.8) and (A.9), we thus have $a^{(k)}(t_0-) = p^{(k)}$.

In the case (ii), from Lemma A.8, $\frac{\mathrm{d}^+}{\mathrm{d}t}u^{(k)}(t_2) + \frac{\mathrm{d}^+}{\mathrm{d}t}w^{(k)}(t_2) = 0$ for every $t_2$ such that $T^{(k)}_{m,n} \le t_2 < T^{(k)}_{m,n+1}$. Thus, from Lemma A.9, (A.8) and (A.9), we have $a^{(k)}(t_0) = 0$. We next show $a^{(k)}(t_0-) = p^{(k)}$. To do so, we first show $\tilde{t} < t_0$ in this case. Suppose $\tilde{t} = t_0$. We then have $f^{(k)}_{m,n} = 0$. On the other hand, from the condition 3, there exists $t_2$ such that $f^{(k)}(t_2) > 0$ and $T^{(k)}_{m,n} < t_2 < T^{(k)}_{m,n+1}$. From Theorem 3.1, we see that those are contradictions, because $a^{(k)}(t)$ has a discontinuous point $t_3$ in the $(m,n)$-cycle such that $a^{(k)}(t_3-) = 0$ and $a^{(k)}(t_3) = p^{(k)}$. Thus, we have $\tilde{t} < t_0$ in this case. From Property A.5, we then have $f^{(k)}(t_0-) > 0$. Therefore, from (A.8) and (A.9), we have $a^{(k)}(t_0-) = p^{(k)}$.

**Acknowledgment**

The work of the third author was supported in part by Research for the Future Program of Japan Society for the Promotion of Science under the Project "Integrated Network Architecture for Advanced Multimedia Application Systems".

**References**

[1] L. S. Brakmo, S. W. O'Malley and L. L. Peterson: TCP Vegas : New techniques for congestion detection and avoidance. *Proc. SIGCOMM '94*, (1994) 24–35.

[2] C. Chase, J. Serrano and P. J. Ramadge: Periodicity and chaos from switched flow systems: Contrasting examples of discretely controlled continuous systems. *IEEE Trans. on Automatic Control*, **38** (1993) 70–83.
[3] C. Fang, H. Chen and J. Hutchins: A simulation study of TCP performance in ATM networks. *Proc. IEEE GLOBECOM '94*, (1994) 1217–1223.
[4] V. Jacobson: Modified TCP congestion avoidance algorithm. end2end-interest mailing list, (1990).
[5] G. Pecelli and B. G. Kim: Dynamic behavior of feed back congestion control schemes. *Proc. IEEE INFOCOM '95*, (1995) 253–260.
[6] M. Perloff and K. Reiss: Improvements to TCP performance in high-speed ATM networks. *Commun. of the ACM*, **38** (1995) 90–109.
[7] A. Romanow and S. Floyd: Dynamics of TCP traffic over ATM networks. *IEEE J. Select. Areas Commun.*, **13** (1995) 633–641.
[8] S. Shenker, L. Zhang and D. Clark: Some observations on the dynamics of a congestion control algorithm. *ACM Comp. Commun. Rev.*, **20** (1990) 30–39.
[9] W. R. Stevens: *TCP/IP illustrated, volume 1: The protocols* (Addison-Wesley, 1994).

Fumio Ishizaki
Department of Information Science and Intelligent Systems,
Faculty of Engineering, The University of Tokushima
2-1 Minamijosanjima, Tokushima 770-8506, Japan
E-mail: `ishizaki@is.tokushima-u.ac.jp`

Tetsuya Takine
Department of Applied Mathematics and Physics,
Graduate School of Informatics, Kyoto University
Kyoto 606-8501, Japan
E-mail: `takine@kuamp.kyoto-u.ac.jp`

Yuji Oie
Department of Computer Science and Electronics,
Faculty of Computer Science,
Kyushu Institute of Technology
680-4 Kawatsu, Iizuka, Fukuoka 820-8502, Japan
E-mail: `oie@cse.kyutech.ac.jp`